Article:
Tsavdaridis, KD and D'Mello, C (2012) Vierendeel Bending Study of Perforated Steel Beams with Various Novel Web Opening Shapes, through Non-linear Finite Element Analyses. Journal of Structural Engineering, 138 (10). 1214 - 1230 . ISSN: 0733-9445

https://doi.org/10.1061/(ASCE)ST.1943-541X.0000562

Vierendeel Bending Study of Perforated Steel Beams with Various Novel Web Opening Shapes, through Non-linear Finite Element Analyses

Konstantinos-Daniel Tsavdaridis[1*], Cedric D'Mello[2]

[1] *School of Engineering and Mathematical Sciences, City University London, EC1V 0HB, UK, Office: C354, E-mail: konstantinos.tsavdaridis.1@city.ac.uk*

[2] *School of Engineering and Mathematical Sciences, City University London, EC1V 0HB, UK, Office: C173, E-mail: C.A.Dmello-1@city.ac.uk*

ABSTRACT

The Vierendeel mechanism is always critical in perforated steel beams with single large web openings, where global shear forces and Vierendeel moments co-exist. Thus far, the main parameters that are known to affect the structural behavior of such beams are the depth of the web opening, the critical opening length of the top tee-section and the web opening area. A comprehensive Finite Element (FE) study of four sizes of perforated steel sections with three different sizes of eleven standard and novel non-standard web opening shapes was undertaken, and their primary structural characteristics presented in detail in order to provide a simple design method for general practice. The different geometric parameters were isolated and studied in order to understand the significance of their effects and in turn advance the knowledge on the performance of perforated steel beams.

An elaborate FE model was established, with both material and geometrical non-linearity, allowing load redistribution across the web openings and formation of the Vierendeel mechanism. The reduction of the global shear capacities, due to incorporation of the local Vierendeel moments acting on the top and bottom tee-sections, was obtained directly from the FE analysis. Following that, a comparison of the global shear-moment (*V/M*) interaction curves of the steel sections with various web opening shapes and sizes was established and empirical generalized *V/M* interaction curves developed. Moreover, the accurate position of the plastic hinges was determined together with the critical opening length and the Vierendeel parameter.

This work has now shown that the shape of the web opening can also significantly affect the structural behavior of perforated beams, as opposed to the equivalent rectangular shape predominately used so far. In addition, the effect of the position of the web opening along the length of the perforated beam was revealed. The importance of the parameters that affect the structural performance of such beams is illustrated. The thorough examination of the computational results has led to useful conclusions and an elliptical form of a web opening is proposed for further study. The outcome of this study is considered as being relevant for practical applications.

Key words: Cellular Beams, Various Standard and Non-standard Web Openings, Novel Shapes, Shear Resistance, 'Vierendeel' Mechanism, Experimental Work, Parametric FE Study, Non-linear FEM, Shear-Moment Interaction Curves, 'Coupled' Shear Capacity Ratios, Utilization Ratios, Plastic Hinges, Critical Opening Length, Stress Concentration Points

Introduction

Requirements for maximum space utilization, efficiency during construction and cost-effectiveness demand the use of long-spanned, shallow, light-weight steel beams in steel and composite structures. In modern building construction spans are becoming longer and one way of achieving this is to use perforated beams. In the last

decade researchers have tried to optimize web opening shapes, sizes and web opening positions in perforated steel beams, in order to provide a better understanding of the stress distribution in the vicinity of the web openings and to examine the structural behavior under certain types of loading. The scope was (a) to provide the maximum possible web opening area for the integration of services (i.e. minimum self-weight), (b) to use long span beams minimizing the number of columns and supports as well as leading to a more efficient use of internal space, (c) to enhance the structural behavior of the final perforated beam under various failure modes and (d) to improve the manufacturing procedure of such steel members (i.e. lower fabrication cost and cost savings in terms of steel material). (a), (b) and (c) are addressed in this research paper; (d) is discussed in a complementary work (Tsavdaridis 2010).

This paper reports on an investigation into three main categories of web opening shapes, typically used (e.g. circular and hexagonal), elliptical and elongated web openings, all with three different hole sizes, 50%, 65% and 80% of the beam's total depth (note: the maximum found in the literature is 75%). Thus, novel non-standard web opening shapes were proposed and comprehensively modeled in order to establish and determine the parameters that influence the structural behavior. In this work, mid-range universal beams were used in order to cover a practical range of beams. Deep web openings are mainly presented throughout this research paper as they represent the worst case scenario, and hence high Vierendeel bending forces are generated in the vicinity of the web openings.

The research work reported here is divided into the following parts:

1. Experimental work conducted in the literature presented herein to compare and validate the FE models and the type of analysis.
2. Development of a FE model followed by a parametric FE study of different perforated beams under Vierendeel mechanism.
3. Development of design *V/M* interaction curves using FE results.
4. Detailed study of the geometric parameters which affect the Vierendeel mechanism.
5. Development of a simple design (step-by-step) method for general practice.

Literature review

As reported by Bower 1968, Redwood and McCutcheon 1968, Lawson 1987; Darwin 1990; Redwood and Cho 1993; Oehlers and Bradford 1995, the presence of web openings may have a severe penalty on the load carrying capacities of structural members, depending on the shapes of the web openings. Many researchers have experimentally studied perforated beams with various standard web opening shapes. Web opening shapes mainly found in the literature are hexagonal (in some cases with an extra mid-depth plate which then creates an

octagonal shape), circular; rectangular; square or elongated (i.e. 'extended'). It was remarkable to note that octagonal web openings behave better than hexagonal ones and that they are easier to manufacture than circular web openings. From FE studies it is also seen that web openings with rhomboidal shapes lead to lower stresses (but concentrated at the sharp corners) than circular ones, due to the narrower opening length at the top and bottom tee-sections. However, the majority of the previous studies were based on global analyses with a combination of forces acting on the perforated beams. Therefore, many parameters were included simultaneously and so unpredicted failure modes were obtained, without being able to tell which parameter affects the results in every particular case. It is now believed that various standard as well as non-standard web openings need to be further investigated on perforated beams with isolated (i.e. single) web openings.

Vierendeel mechanism

This mode of failure is associated with high shear forces acting on the beam. Formation of plastic hinges at the corners of the web opening shapes and/or at specific positions (φ_p angles) deforms the tee-sections above the web openings to a stretched shape. This mode of failure was first reported by Altifillisch et al. 1957; Toprac and Cook 1959, regarding castellated beams and Redwood and McCutcheon 1968, regarding cellular beams.

When a perforated steel beam is subjected to shear, the tee-sections above and below the web openings must carry the applied shear as well as the primary and secondary moments. The primary moment is the convectional bending moment and the secondary moment, also known as the Vierendeel moment, results from the action of shear force in the tee-sections over the horizontal length of the web opening. Therefore, the horizontal length of the web opening directly affects the secondary moment. In the absence of local or overall instability, perforated beams with standard web openings have two basic modes of collapse, which depend upon the geometry and the position of the web opening. They are as follows:

- Plastic tension and compression stress blocks in the top and bottom tee-sections in regions of high overall buckling.
- Parallelogram or Vierendeel action due to the formation of plastic hinges at the four corners or at specific angles around the web opening, in regions of high shear.

More analytically, the presence of a single (i.e. isolated) web opening in a steel beam introduces three different modes of failure at the perforated beams:

1. Flexural failure due to reduced moment capacity.
2. Shear failure due to reduced shear capacity.
3. Vierendeel mechanism (**Fig. 1**) under the Vierendeel action.

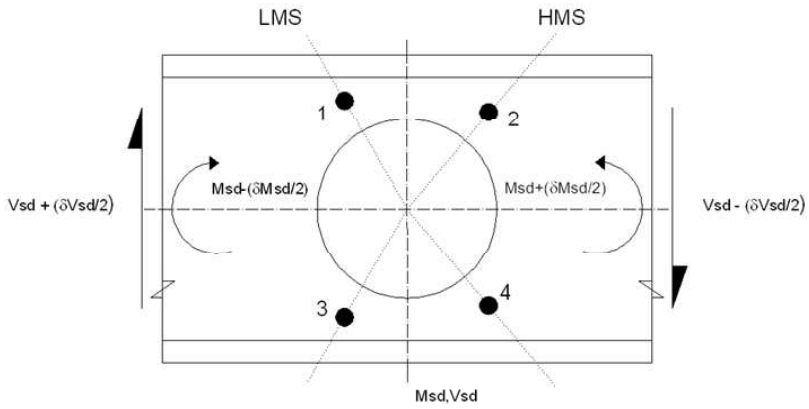

Fig. 1: Vierendeel mechanism and location of plastic hinges (Chung et al. 2000)

There are two design methods in assessing the structural behavior of steel beams with web openings: (i) the perforated section approach and (ii) the tee-section approach. The first method was used in this research paper.

Objectives

In this investigation the Vierendeel failure mechanisms of steel beams with web openings are examined through an extensive FE study. It is known that the shear and flexural failures of standard perforated sections are controlled mainly by the size (i.e. depth) of the web openings, whilst the Vierendeel mechanism is primarily controlled by the critical length of the web openings at the top and bottom tee-sections.

This research work aims to:

- Introduce web opening shapes with a maximum depth equal to 80% of the beam's depth. The purpose of this is to either lighten the beams (i.e. larger cut-outs) or to increase their final depth and so their second moment of area, following the typical profile cutting manufacturing procedure.
- Propose ideal effective novel non-standard web opening shapes in terms of structural performance.
- Investigate the Vierendeel mechanism in steel perforated beams with various standard and novel non-standard web openings.
- Perform parametric studies on mid-range steel beams and draw the non-dimensionalized 'coupled' shear-moment interaction curves.
- Isolate and examine the geometrical parameters which influence the structural behavior of the perforated beams in order to understand the significance of their effects and in turn enhance the performance of perforated beams.
- Compare the structural behavior of the novel beams with the typical perforated beams.

- Revise an empirical design method by using generalized non-linear *V/M* interaction curves.

This paper focuses on the structural improvement of the steel perforated beams with the scope to develop light-weight steel members. The idea is to design perforated beams with web openings which provide the maximum possible web opening area for the integration of services and the minimum self-weight; hence low deflections, utilizing the minimum possible web opening spacing (i.e. increase the number of web openings located adjacent to each other).

Methodology

Initially, the results of an experimental programme of work found in the literature (Redwood and McCutcheon, 1968) were used to validate the FE model. An elaborate FE model was established with both material and geometrical non-linearity in order that load redistribution across the web openings occurs and formation of the Vierendeel mechanism could take place following the re-arrangement of the plastic hinges. The interaction effects of the overall shear force and overall bending moment were investigated.

The load carrying capacities of universal steel beam sections (UB sections from Corus) were examined and the results non-dimensionalized. It is important to mention that the beam analyzed consisted of only one web opening on each half-span, with the position of the web opening being changed along the length of the beam in order to obtain different shear-moment ratios at the center-lines of the web openings. In the case that web openings are aligned next to each other, a combination of forces will act in the vicinity of the web openings and Vierendeel study would become impossible. In the latter case, the web-post buckling failure modes will dominate (Tsavdaridis and D'Mello 2011). The outcome of the current study assumes that a minimum required web opening spacing is provided according to the design rules. Also, it should be noted that the web openings of the beams tested and analyzed were formed by cut-out manufacturing procedures and not from profile cutting, as in the latter case the large number of variables would have resulted in very complex analyses (eg. with different final section depths and web opening spacing).

The exact position (φ_p angles) of the plastic hinges in the vicinity of the web openings is an important consideration. Consequently, the geometrical parameters which influence the structural behavior of the perforated beams under Vierendeel actions were thoroughly investigated. (Tsavdaridis 2010; Tsavdaridis and D'Mello 2009)

Validation of the FE model with experimental work

FE model

The finite element model was validated against the test data of two steel I-section beams of different spans with single circular web openings, as reported by Redwood and McCutcheon (1968). The test specimens with their geometrical details are depicted in **Fig. 2**.

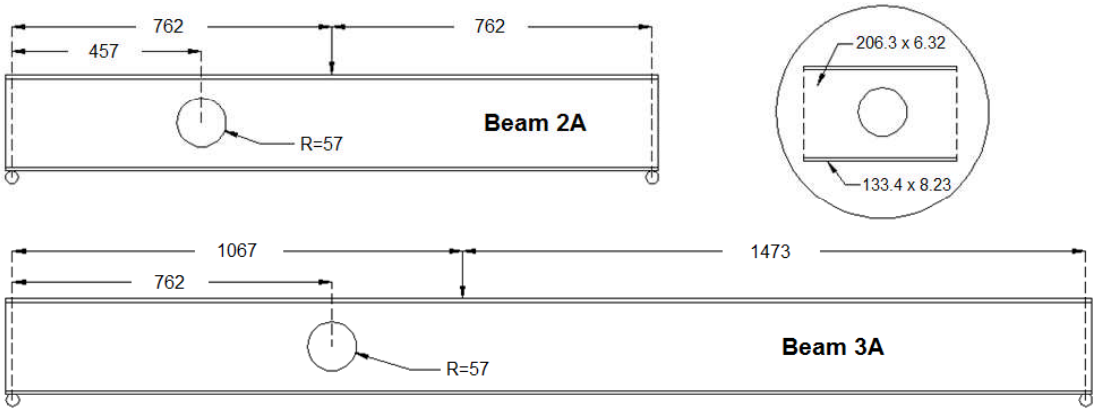

Fig. 2: Geometrical properties of the test specimens (all dimensions in mm)

In order to simulate the structural behavior of the experimental setup, a finite element model was developed in a commercial FE analysis software package, ANSYS v11.0, which incorporated material non-linearity, and hence the beam model was capable of mobilizing the moment capacities of the tee-sections under co-existing axial and shear forces due to global action. The elastic modulus, E, was assumed to be 200GPa. A bi-linear stress-strain curve was used in the material modeling of steel together with the Von-Mises yield criterion and the kinematic hardening rule, which is suitable for most metals including steel. Geometric non-linearity was also used; hence a large displacement static option was incorporated in the model allowing load redistribution in the web across the web openings after initial yielding. The previous allow the Vierendeel mechanism with the formation of four plastic hinges in both the tee-sections above and below the web openings. The material properties of the steel beams as reported by Redwood and McCutcheon (1968) are presented in Table 1 below.

Table 1: Material properties of the steel beams taken from coupon tests

Mesh convergence

Mesh convergence is one of the most overlooked issues that affect accuracy of the FE models. The rate of change of stress is dictated by the rate of change of load or geometry in the region of interest. In the subsequent

models the most interesting areas are the vicinity of the web openings and the actual element size was carefully considered.

A maximum element size of 25mm was chosen for the meshing of the area in the vicinity of the web openings. No attempt was made to use a finer element because a transition region would be necessary and this would be a time consuming study. It is worth mentioning that the error estimation for the displacements was satisfied better with mesh refinement compared to the error of the stresses, since a 4-noded element was used.

Meshing

In **Fig. 3** the FE model of the 2A test is illustrated, where the flanges and the web of the steel beam are modeled with iso-parametric 4-noded quadrilateral plastic shell elements (SHELL181). A circular web opening was formed in the web with refined mesh configuration in order to avoid discontinuities in stress contours across element boundaries. The same element size and type was used for the 3A test specimen as well.

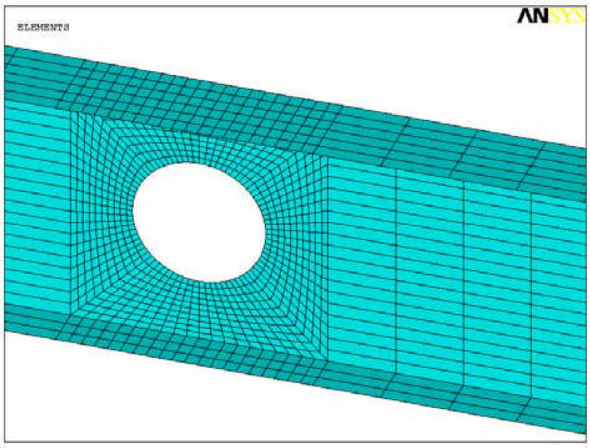

Fig. 3: Detailed meshing of the perforated steel beam

Following the sensitivity studies on both the configuration and the density of the finite element mesh, it was found that over 6,050 shell elements were required to model the flanges, the web, the bearing plates at the supports and the web stiffeners, while 1,800 of these shell elements were located around the web opening. Respectively, the number of shell elements that were required for the 3A test specimen after the sensitivity studies were 7,550 along the whole beam while, 1,800 of these shell elements are located around the web opening, as the 2A specimen. It is clearly noticeable that the total number of elements for the longer beam, 3A, was not dramatically increased because there are no web openings on the right hand side of the beam. Therefore, coarser elements were utilized. The full Newton-Raphson solution procedure was also used to analyze the beam during the entire deformation history.

During the numerical investigation, it was necessary to ensure that the finite element models failed only at the perforated sections, similar to the corresponding tests, and failure in other parts of the beam including overall instability was restricted. Moreover, the web openings were free from any boundary effects or point loads.

FE Results

For both tests, the bending moment against mid-span deflection curves obtained from the finite element modeling are plotted in **Fig. 4** together with the measured test data from the literature for a direct comparison. It is shown that both the maximum moment capacities of the perforated sections and the deformation characteristics of the beams are modeled satisfactorily. This provides confidence in the use of the developed FE model.

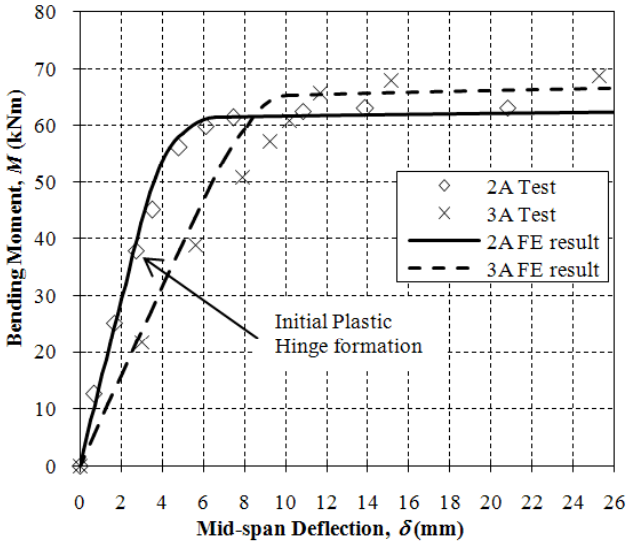

Fig. 4: Comparison of load-deflection curves for tests 2A and 3A

It is interesting to examine the stress distribution of the perforated beams at both first yield and failure conditions for instance of Beam 2A, as shown in **Fig. 5**. As is depicted in **Fig. 5**, the first yield approximately appeared in the web of the tee-sections at cross sections with $\varphi=30^o$ and $\varphi=45^o$ from the vertical center-line of the web opening. Observing the Von-Mises stresses at failure point, both the webs and the flanges of the tee-sections at the high moment side (HMS) have extensively yielded. However, at the low moment side (LMS), only the webs of the tee-sections have yielded, while the stress level of the flanges reaches around 70% of the yield strength of the HMS. Finally, as shown, Beam 2A failed with the formation of four plastic hinges, two of them fully at HMS and another two partially at LMS. Beam 3A starts to yield later than Beam 2A and the top flange at the HMS of

the perforated section buckles locally under large global bending action, as the location of the web opening gives rise to a different shear-moment ratio.

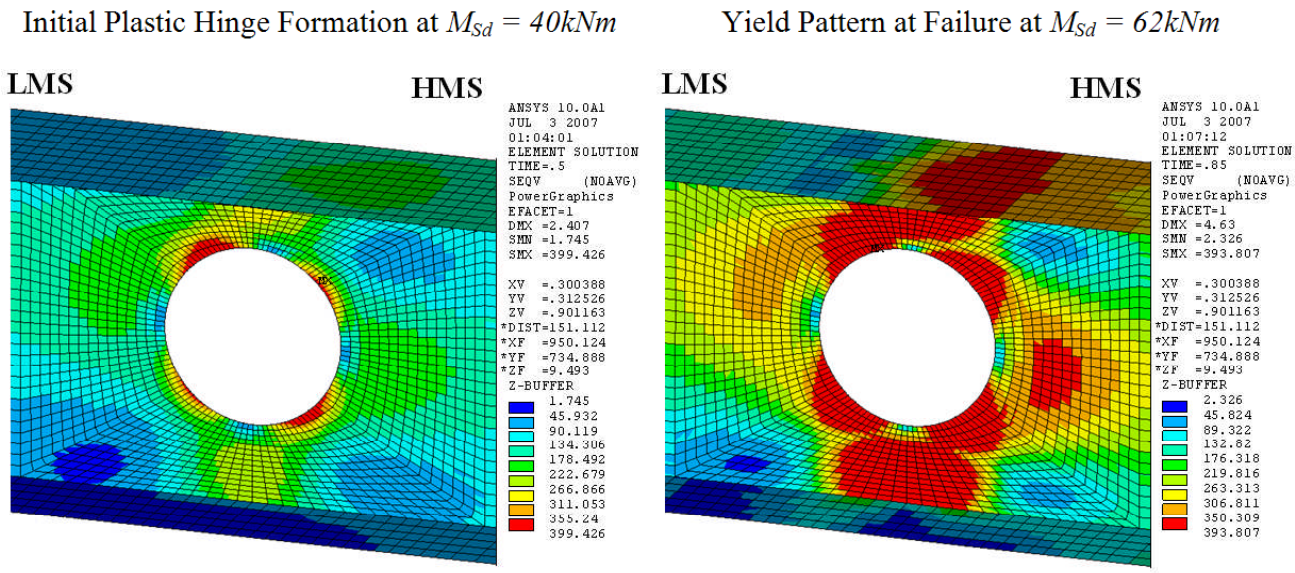

Fig. 5: Von-Mises stress distribution at perforated section in Beam 2A

Parametric FE study of various web opening shapes and sizes

Web opening shapes

The FE method was used to examine the behavior of full scale steel beams with two large isolated openings in the web, symmetrical about the mid-span center-line. To compare the efficiency of the various shapes of web openings, eleven forms were considered, six of these being standard configurations, including elongated web openings, whilst the other five were elliptical web openings (**Fig. 6**). Details of the aforementioned web opening shapes together with the associated values of the uniform tee-section (i.e. critical opening length, c,) are listed below:

1. Circular opening with $c < 1.0d_o$ (A)
2. Regular hexagonal (60^o angle) opening with $c = 0.423d_o$; sharp corners where the stresses are always concentrated (B)
3. Vertical ellipse with width size 75% of its depth and with $c < 0.75d_o$ (C)
4. Inclined ellipse with width size 75% of its depth, rotated by 45^o about the centroid of the web opening and with $c < 1.0d_o$

Rotating the vertical ellipse C, its vertical opening depth is shorter compared to the height of the I-section. Three beam configurations were studied with different web opening orientations presented as

follows: the symmetrical web openings are mirrored to the mid-span of the beams whilst rotated by 45° (D & E) about the centroid of the web openings and the case that both symmetrical web openings are rotated by 45° in only one direction (F). The three different options are presented in **Fig. 6** (right). It was expected to have a variation of the critical opening length, *c*, of the top and bottom tee-sections when perforated beams with inclined web openings are used. Also, the scenario of web openings asymmetrically aligned to the mid-span (F) was of great interest.

5. Inclined (rotated) ellipse with $c < 1.0d_o$; its vertical opening depth, d_o, is equal to *0.8h* (G)
6. Square opening circumscribed about the circle and $c = 1.0d_o$ (H)
7. Elongated circular opening with $1.0d_o < c < 2.0d_o$ (I)
8. Rectangular opening with $c = 2.0d_o$ (J)
9. Ultimate elongated circular opening with $2.0d_o < c < 3.0d_o$ (K)

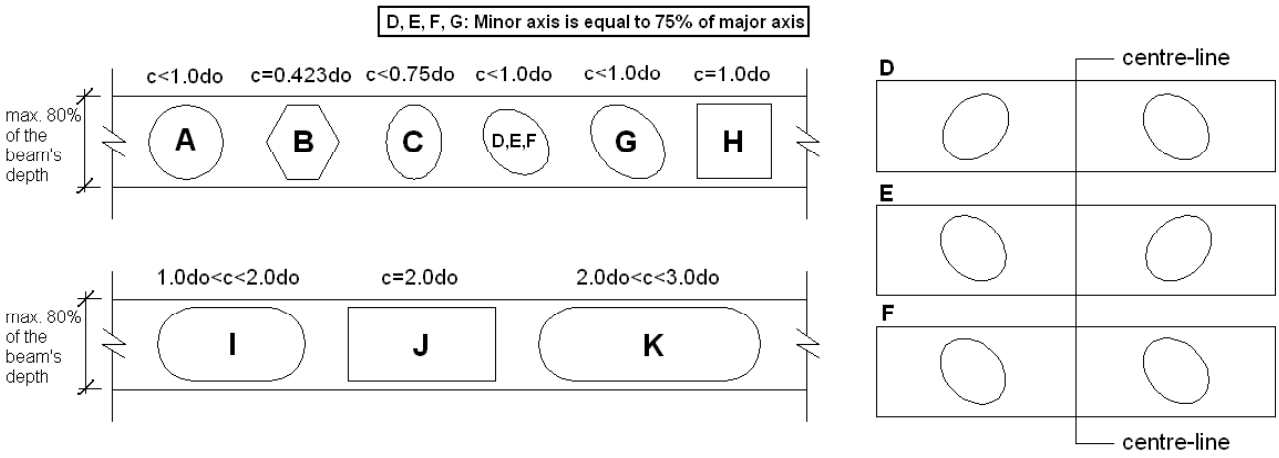

Fig. 6: Geometric configurations of web openings (left) and rotated elliptical web openings (right)

It is worth mentioning that, in order to find the critical opening length, *c*, for each web opening configuration, the Von-Mises stress concentration points at the top tee-section need to be considered at the failure load and when the web opening of the perforated section is under high shear forces (i.e. $M_{o,Sd}=0$). **Table 4** provides detailed information for the exact position of the plastic hinges (i.e. stress concentration points).

Summary of FE model

The aim of the comparison between the FE model and the experimental tests from the literature was to ensure that the elements, material properties, real constants and convergence criteria were adequate to model the response of such perforated steel members. The summary of the FE procedure which was used for the parametric studies on Vierendeel mechanism is as follows:

- Use of 4-node shell (SHELL181) elements with a quadratic deformation approach; same results obtained using SOLID45 (8-node element).
- The influence of meshing and its refinement was addressed through convergence study, such that the presented FE results can be regarded as consolidated.
- Geometrically as well as material non-linear interaction.
- Solver by iterations according to Newton-Raphson.
- Nominal material properties were used for steel grade S275.
- A bi-linear stress-strain curve with a Young's Modulus, E, of 200GPa and a Tangent Modulus, E_T, of 1000MPa was used, together with a bi-linear kinematic hardening rule and the Von-Mises yield criterion (**Fig. 7**).
- Bearing plates at the two ends of the beam were modeled and the pressure was directly applied to the compression flange of the beam.
- The load was applied stepwise as pressure.

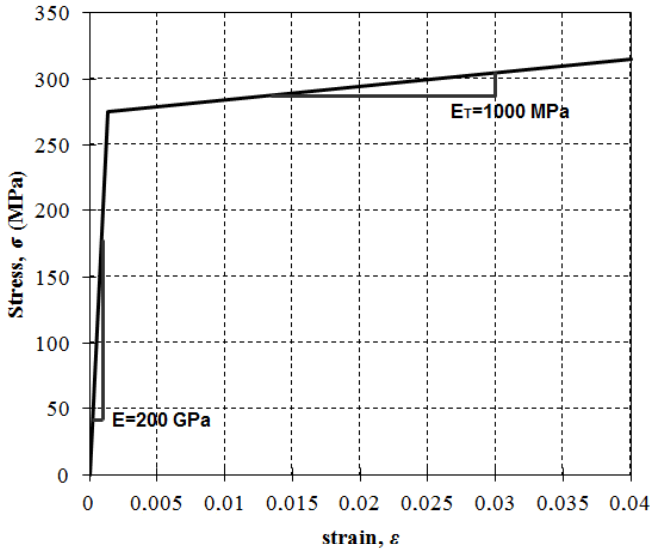

Fig. 7: Idealized bi-linear stress-strain curve

Study model

Non-linear shear-moment interaction curves are used to present the results of this investigation. The FE model using both geometrical and material non-linearity allowed load redistribution across the web opening following the formation of the first plastic hinge (i.e. stress concentration point). According to Chung et al. (2003) four typical mid-range steel beams commonly used in practice can be investigated in order to obtain useful results. From comprehensive FE analyses conducted by the authors of this paper on beams

UB457x152x52, UB457x152x82, UB610x229x101 and UB610x229x140, the mid-range beam size UB457x152x52 was selected to represent this study as it produced the most conservative results. Also, UB457x152x52 has a web thickness of 7.6mm which makes the beam susceptible to web buckling and so makes it more likely to buckle locally and form plastic hinges. 1320 successful non-linear FE runs were conducted in order to complete this parametric study. Establishing shear-moment interaction curves, ten different positions (x) of the web openings along the length of the beam were considered appropriate. The load carrying capacity comparisons of perforated sections with beams of different spans (5, 6, 7.5 and 10m), having various web openings sizes (d_o equal to *0.5h* and *0.75h*) was examined (Tsavdaridis 2010; Chung et al. 2000). In detail, when perforated beams with small web openings are considered, it is noticed that there is no significant reduction in the shear capacity with any beam span. Some reduction in the load carrying capacity is the result of the reduced moment capacity close to the mid-span of the beams, where the Vierendeel action is not critical. The area of this reduction is approximately 1/3rd of the beam's span and it is of a higher magnitude in short span beams. On the other hand, when perforated beams with large web openings are considered, the combination of the beam span and the web opening position could yield completely different results. For long span beams (>7m) and web openings located close to the mid-span, the beams tend to fail in flexure due to a reduced moment capacity. However, for short span beams a reduced load carrying capacity is obtained when the web openings are located either close to the supports or close to the mid-span. For conservative reasons, short-span simply-supported perforated beams with a span of 5m under a uniformly distributed load were modeled, as the fluctuation of the results using large web openings leads to important conclusions. Two specific locations labeled as positions x equal to 1 at support and 10 at mid-span were under significant consideration. The perforated section at position 1 was under pure shear, while the perforated section at position x equal to 10 was under pure moment.

Shear/Moment (V/M) interaction curves

A simple design method proposed in the literature (Chung et al. 2003), is related to 'coupled' shear capacities and allows for the Vierendeel mechanism. The behavior of perforated sections is characterized by three actions: global bending action, global shear action and local Vierendeel action. The shear-moment interaction curves for UB457x152x52 (S275) obtained from the finite element investigation are presented in **Fig. 8**, where the vertical axis is the 'coupled' shear capacity ratio (**Eqs. (5)**) and the horizontal axis is the 'coupled' moment capacity ratio (**Eqs. (6)**). At failure, the global shear force, $V_{o,Sd}$ (**Eqs. (1)**) and the global moment, $M_{o,Sd}$, (**Eqs. (2)**) at the center-line of the openings, are non-dimensionalized with respect to the global section capacities of the perforated sections, $V_{o,Rd}$ and $M_{o,Rd}$, **Eqs. (3)** and **Eqs. (4)**, respectively. The load w is taken directly from FEA.

$$V_{o,Sd} = w\left(\frac{L}{2} - x\right) \quad (1)$$

$$M_{o,Sd} = wx\frac{(L-x)}{2} \quad (2)$$

$$V_{o,Rd} = f_v A_{vo} \geq V_{Sd}, \quad A_{vo} = A_v - d_o t_w, \quad f_v = \frac{0.577 f_y}{\gamma_{Mo}} \quad (3)$$

$$M_{o,Rd} = f_y W_{o,pl} \geq M_{Sd}, \; W_{o,pl} = W_{pl} - \frac{d_o^2 t_w}{4} \quad (4)$$

"The 'coupled' shear capacity governs the global shear capacity of a perforated section under 'coupled' shear failure and Vierendeel mechanism, in the absence of global moment."(Chung et al. 2003) The 'coupled' shear capacity ratio, $\overline{v}$, for perforated sections is defined as follows:

$$\overline{v} = \frac{V_{o,Sd(FEA)}}{V_{o,Rd}} \quad (5)$$

The corresponding 'coupled' moment capacity ratio, $\overline{m}$, for perforated sections is defined as follows:

$$\overline{m} = \frac{M_{o,Sd(FEA)}}{M_{o,Rd}} \quad (6)$$

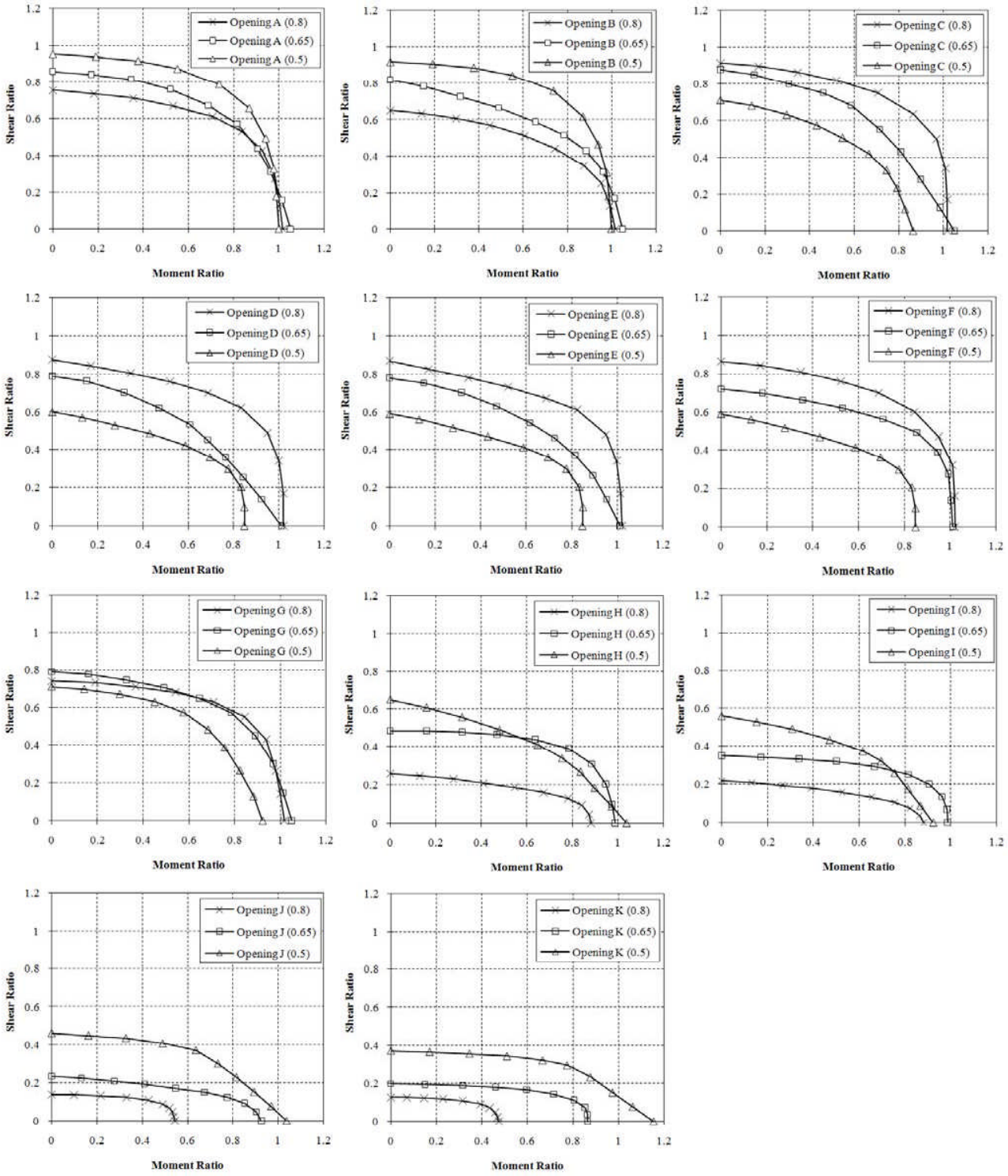

Fig. 8: Non-dimensional *V/M* interaction curves for various web opening shapes and sizes

All interaction curves are generally similar in pattern and therefore allow for an application of a generalized shear-moment interaction curve for practical design. For web openings with the same values of d_o but with different values of c, the load capacities of the perforated sections should be inversely proportional to the values of c. Regarding all elliptical web openings, it is found that as the web opening size becomes bigger the shear ratio increases, inversely to the typical beams. The explanation for this is given below, relating the load capacity with the assumption of the shear cross sectional area in the global section capacity formula.

As anticipated, the reduction in the shear capacity is more pronounced when compared to the reduction in the moment capacity as the presence of the web opening reduces the shear area of the section significantly but the reduction of the plastic section modulus is small. At times, it is noticed that the moment ratio is slightly higher than 1.0. However, significant reduction of the moment capacity is obtained for perforated beams with elongated web openings.

First category – (Standard typical A and B): Perforated sections in this category behave normally. The bigger the web opening size the lower the shear ratio is. Independent of the web opening size in all cases, all moment ratios are similar. The percentage of reduction for perforated sections with web openings under high shear forces is the same among the three sizes of web openings.

Second category – (Non-standard elliptical C, D, E, F and G): Perforated sections with vertical and inclined ellipses behave similarly to the typical web opening configurations. As the latter have a narrow opening length, especially when vertical elliptical web openings are considered, the effects due to Vierendeel action are insignificant.

When comparing the FEM curves between circular and inclined elliptical web openings it is found that the rotation of an elliptical web opening causes dissimilar reduction of the shear-moment ratios. Perforated sections with various web opening sizes are affected differently by the web opening rotation parameter. The reduction of the web opening depth affects the shear and moment capacities of the perforated sections (i.e. the denominator of 'coupled' shear and moment capacity ratios – **Eqs. (5)** and **(6)**). Also, the load carrying capacities of the perforated sections are now similar, independent of the web opening size (i.e. the nominator of 'coupled' shear and moment capacity ratios – **Eqs. (5)** and **(6)**). This is due to the critical reduction in depth of the larger web openings, and the geometry of the particular asymmetrical web opening shapes, which results in a different combination of forces acting on the top and bottom tee-sections. An uneven stress distribution in the vicinity of elliptical web openings was evidently observed. As a result, perforated beams with large elliptical web openings present a dramatically increased capacity due to a narrower opening length and a decreased web opening depth compared to the circular web openings. Inversely, most affected are the perforated sections with web openings of d_o equal to $0.5h$, where both the x- and y-intercepts of the FEM curves are reduced as their load carrying

capacity is relatively low compared to the web opening size. The latter characteristics result in the significant re-arrangement of the shear-moment ratios.

In summary, the web opening shape (because of the increased load carrying capacity, especially for large ellipses with a narrow opening length), and the web opening rotation (i.e. same web opening area and so beam weight with shorter web opening depth), are the main parameters which cause dissimilar reduction of the 'coupled' shear and moment ratios when elliptical web openings are considered.

Inclined elliptical web openings (G) with d_o equal to *0.8h*, *0.65h* and *0.5h*, after rotation, present similar shear-moment ratios, and the overall behavior is like the other perforated sections with elliptical web openings. The y-intercepts of the FEM curves are closer in this case as there is no reduction of the opening depth, d_o, for this web opening shape. It should be noted that, the area of the maximum web opening is only 5.8% smaller than the area of the typical circular web openings (A), whereas the d_o are the same. Moreover, when comparing the structural performance of these two perforated sections it can easily be concluded that apart from the opening length, *c*, the web opening shape also controls the performance due to the movement of the stress concentration points.

Third category – (Non-standard elongated H, I, J and K): In these perforated sections the size of the opening length dramatically affects their structural behavior. Perforated sections with relatively large web openings H and I have FEM curves of similar pattern and relatively close moment ratios. Moreover, perforated sections with dramatically elongated web openings J and K have FEM curves of similar patterns, while the moment ratios also significantly change depending upon the web opening size. It is observed that perforated sections with the elongated web opening shapes and d_o equal to *0.8h* present considerably reduced moment ratios when the web openings are located at a high moment region, unlike to other opening types. The important reduction of the moment ratios dominant in this category is justified by the existence of four high bending moments applied on perforated sections with large web openings located close to mid-span, as opposed to two plastic hinges found for the rest of the web opening shapes examined.

'Coupled' shear capacity ratios allowing for Vierendeel mechanism

The global 'coupled' shear capacities of perforated sections covered in the present study, allowing for Vierendeel mechanism, are obtained directly from the shear-moment interaction FEM curves as presented in **Fig. 8**. **Table 2** summarizes the values of the maximum 'coupled' shear capacity ratios, $\bar{v}$, for perforated sections with web openings subjected under pure shear forces (i.e. position x equal to 1).

Table 2: Summary of maximum 'coupled' shear capacity ratios, $\bar{v}$

Comparison of V/M ratios of various section sizes

Furthermore, a comparative study was established between the four mid-range sections sizes of the universal beams with selected web opening shapes of maximum size. This is done, in order to investigate the difference between the 'coupled' shear capacities by using the following three approaches for the cross section shear area.

- In the simple plastic section analysis, the shear area of an I-section is taken as ht_w (BS5950 Part1:2000) for practical reasons.
- As considered in ENV (1993-1-3) EC3, where the length of the fillet radius between the web and the flange is equal to the effective width of the flange.

$$A_{VZ} = A - 2bt_f + (t_w + 2r)t_f \tag{7}$$

- The proposed equivalent shear area of a tee-section based on a FEA investigation. (Chung et al. 2003), as it was used previously to develop the shear-moment interaction curves.

$$A_v = ht_w + 2\left(0.75t_f^2\right) \tag{8}$$

Typical circular (A), vertical ellipse (C), and elongated (I) web openings are selected to be examined in this study in order to cover all three main categories. The shear-moment interaction curves are presented for ease of comparison (**Fig. 9** to **Fig. 11**) and the results are summarized in **Table 3**.

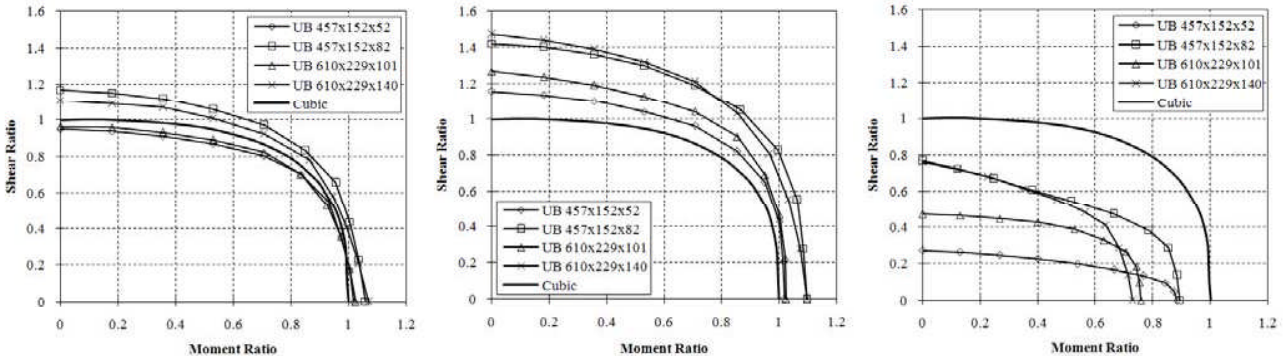

Fig. 9: *V/M* ratios with A_v from BS (Web opening A-left, C-middle and I-right)

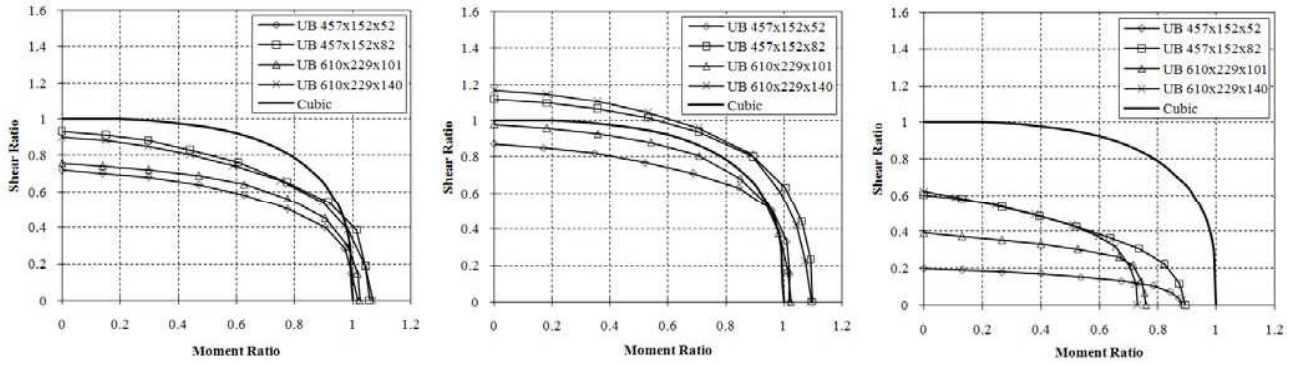

Fig. 10: *V/M* ratios with A_v from EC3 (Web opening A-left, C-middle and I-right)

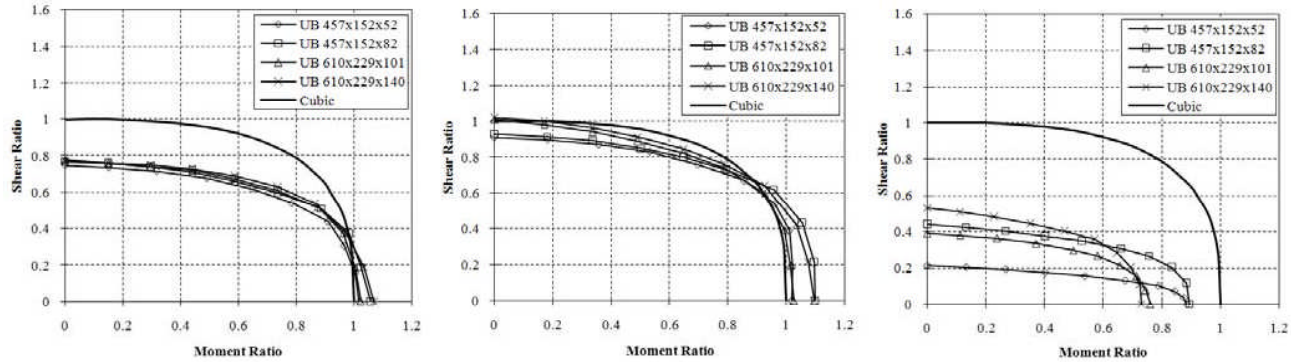

Fig. 11: *V/M* ratios with A_v as proposed in **Eqs. (8)** (Web opening A-left, C-middle and I-right)

Table 3: Comparison of the 'coupled' shear capacity ratios, $\bar{v}$

Studying all the above data, several conclusions are drawn concerning the three approaches for the evaluation of the shear cross sectional area, A_v, and they are given as follows:

- It is observed that beams with the same serial size have a similar 'coupled' moment capacity ratio and only the 'coupled' shear capacity ratio is altered.
- Among beams with the same serial size but with different weights per unit length, the lighter is always the one having a lower 'coupled' shear capacity ratio.
- Among beams of different serial sizes but with the same web thickness, those with the thicker flanges have always higher 'coupled' shear capacity ratios. In most cases, as the ratio t_f/t_w is increased the 'coupled' shear capacity ratio is also increased.

The above latter statement is justified regarding the UB457x152x82 which has the highest t_f/t_w ratio among the particular beam sections. By using the shear area (**Eqs. (8)**), this beam has the maximum decrease in the 'coupled' shear capacity ratio compared to the other beams. From further study, it is observed that the percentage difference is decreased when perforated sections with smaller web opening sizes are considered.

Observing **Table 3** it is also noticed that the maximum deviation of the 'coupled' shear capacity ratios is found between the conventional shear area assumption taken from BS5950 Part1:2000, and the shear area assumption taken from **Eqs. (8)**. On the other hand, 'coupled' shear capacity ratios estimated by using the assumptions from EC3 and **Eqs. (8)**, especially for UB457x152x52 and UB610x229x101, presented very close results. This is due to the small flange thickness which also contributes little to the shear capacity.

Yield patterns

Von-Mises stresses are used to reveal the plastic hinges in the vicinity of the web openings which are formed at both ends of the tee-sections. The positions of these plastic hinges are influenced by the magnitude of the global shear force and bending moment. The shear forces produce additional moments, as first mentioned. By understanding the movement and the critical positions of these plastic hinges, the actual critical opening length can be obtained. It is worth mentioning that a mesh convergence study was initially implemented to assure that the element size would not affect the accuracy of the results. **Fig. 12** and **Fig. 13** show these hinge positions for all examined web opening shapes for UB457x152x52, with web openings of depth equal to *0.8h,* when they are located at a distance, x, equal to 0.284m and 1.866m from the left hand support, respectively.

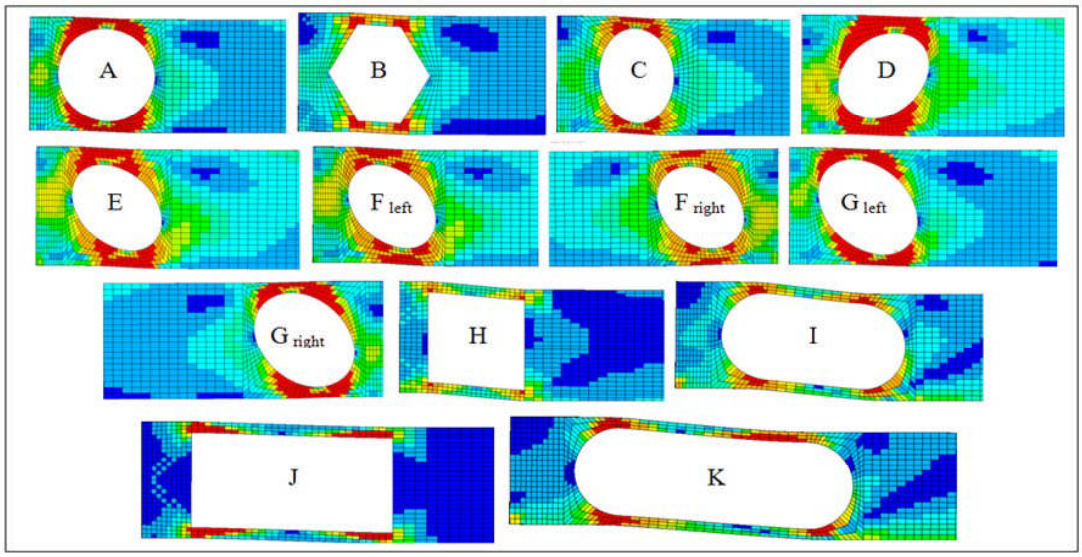

Fig. 12: Von-Mises stresses of beams subjected to high shear forces ($d_o/h=0.8$, x=*0.284m* from support)

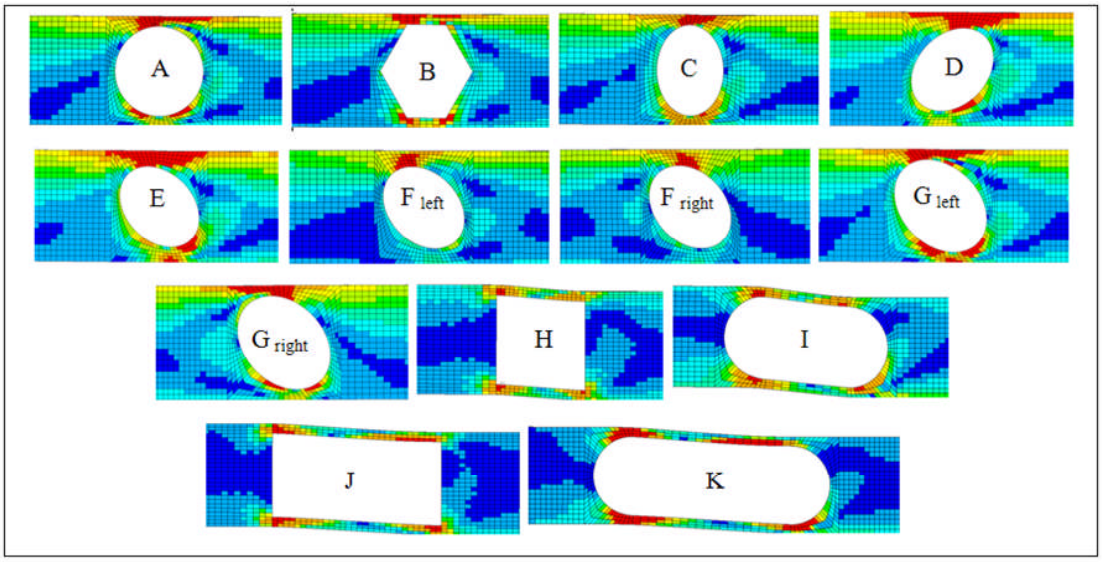

Fig. 13: Von-Mises stresses of beams subjected to high shear forces ($d_o/h=0.8$, x=*1.866m* from support)

The yield patterns for perforated beams with all eleven web opening shapes and three different sizes (d_o equal to *0.8h*, *0.75h* and *0.5h*) are extensively presented by Tsavdaridis (2010), including the stress at the top-compression steel flange in order to draw the complete formation of the four plastic hinges. This FE study found that in the case of non-standard web openings, the structural performance of the perforated sections is strongly affected not only by the opening depth and critical length, but also the web opening shape and not the web opening area.

When the perforated sections are under high global shear force and low global bending moment, the plastic hinges at the LMS and HMS of the perforated sections are shown to be fully developed (**Fig. 12**). Conversely, when the perforated sections are under low global shear force and high global bending moment, plastic hinges at both ends of the tee-sections above and below the web openings are mobilized by the action of large local axial forces (**Fig. 13**). Hence, only the plastic hinges of the LMS of the perforated sections are shown to be fully developed. At the same time highly stressed compression flanges are found on the HMS. It is also observed, that for most of the perforated sections with relatively narrow opening length, *c*, such as perforated sections with web openings A, C, D, E, F and G, the yield zones at both the LMS and HMS of the perforated beams significantly overlap. Generally, it can be concluded that in terms of stress distribution, perforated sections with vertical elliptical and rotated elliptical web openings have a better structural performance compared to circular, hexagonal and elongated web openings. Moreover, when the perforated sections are under pure bending moment, axial forces due to the global bending moment action exist in the tee-sections, and highly stressed top tee-sections are observed. Knowing the position of the plastic hinges when the web openings are located at high

shear regions, the actual critical opening length, *c*, of each web opening is given and is considered for further investigation. For practical purposes the outcome of this study can be considered as very important, since the local buckling point can be pre-determined and enhanced and hence avoid failure of the member.

Finally, it should be noted that an additional high deflection (known as Vierendeel deflection) is observed in perforated sections with square, elongated and rectangular web openings. These perforated sections failed suddenly at low loading levels by excessive element deformation/distortion. This is as a result of high shear forces and Vierendeel bending moments applied on the wide opening length, *c*, of the top tee-section and its elongated shape.

Analytical study of inclined elliptical web opening shapes

Serious consideration is taken to find the most effective orientation of the inclined ellipses (i.e. either D, E or F). It is observed that the overall beam structural performance changes slightly in every case. In the case that the web openings are symmetrically mirrored with regards to the mid-span (i.e. D and E), the behavior is the same at the two ends, thus only one study at one end of the beam is needed. In particular, in perforated sections with web openings E, the plastic hinges initially form at the top tee-section at LMS and then the bottom tee-section at HMS, bottom tee-section at LMS and finally the top tee-section at HMS. Also, plastic hinges form at a low load level point. Conversely, in the case of the perforated section with web openings D, all four plastic hinges almost simultaneously form at a higher load level. When both web opening shape configurations are used is a perforated beam, the structural behavior is less easy to predict.

In more detail, the FEA shows that in cases when loading perforated beams with web openings E, the ellipse is significantly elongated while its minor axis is shortening by stretching the shape due to the additional deflection. Hence, the total displacement of the beam is significantly high. On the other hand, in cases when perforated sections with web openings D, the elliptical shape tends to transform to an approximate 'circular' shape. Therefore, the additional displacement of the perforated section is negligible.

Changing the angle of the inclined web openings gives different results. The depth of the web opening, d_o, and the opening length, *c*, is going to change, leading to different results. The angle of rotation is limited to 45^o in this research paper.

Position of plastic hinges

Previous approaches for circular web openings have approximated the circular web opening as an equivalent rectangle, thereby implying that the critical section is constant and relatively independent of the shear-moment ratio acting on the beam (Redwood 1969; Redwood 1973). However, FE analyses of cellular beams showed that

this is an oversimplification, because the critical section changes according to the shear-moment ratio in the beam.

The angle φ_p of the critical plastic hinge is taken from the LMS and the center-line of the web opening, which usually appears first. After the formation of the first plastic hinge, there is load redistribution across the web opening and the other plastic hinges are formed in a slightly different way. In general, the angle φ_p is increased as the web opening is located closer to the support and the stress is transformed from elastic to plastic under the increased local bending moment, M_φ. Stresses at the top tee-section are more compressive compared to stresses in the flange. The approximate plastic hinge positions at the LMS of the top tee-sections examined in this paper are summarized in **Table 4**, and the critical opening length, c, can then be determined (**Fig. 14**).

Table 4: Angle, φ_p, of the first plastic hinge at top tee-section and LMS following load redistribution

As is shown in **Fig. 14**, the shape of the web opening (i.e. whether symmetrical or not) also significantly affects the position of the plastic hinges which then affects the value φ_p. This is the explanation as to why in the perforated beam with web opening D, the angle φ_p of the plastic hinge is much smaller than the one with web openings E and F, despite the fact that they all have a critical length, c, equal to $0.25d_o$. Furthermore, from the figures below it can be concluded that in perforated beams with elongated web openings as well as hexagonal web openings (generally regular polygons), the angle of the first plastic hinge slightly varies, independently of the web opening positions along the length of the beam, due to the stress concentration at the sharp corners. This is clearly shown in **Fig. 14** (identical points). Also, a linear approximation of the angle, φ_p, can be drawn in **Fig. 14**, regarding the web opening shapes with critical opening length, c, greater than $0.423d_o$.

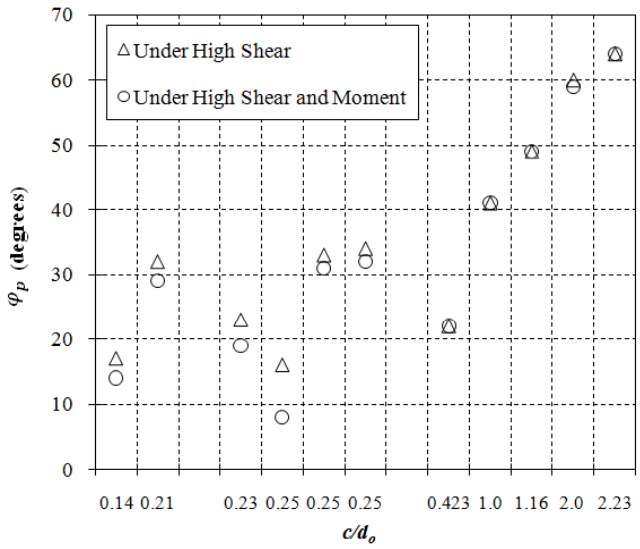

Fig. 14: Angle, φ_p, of the first plastic hinge in respect to c/d_o

Vierendeel parameter

The applied moment at the LMS of the web opening results in tensile and compressive forces in the web-flange sections. These forces are considered for the analysis of the behavior of steel beams and they act at the elastic neutral axes of the sections. The Vierendeel moment across the web opening is resisted by the four plastic moment capacities of the sections, which may or may not be stiffened.

In order to examine the performance of the Vierendeel mechanism in perforated sections, a parameter is established known as the Vierendeel parameter, v_i, (Chung et al. 2003) and is defined as:

$$v_i = \frac{V_{o,Sd(FEA)}}{4M_{T,Rd}/_c} \quad (9)$$

An illustration of the importance of the Vierendeel mechanism in perforated sections with standard and non-standard web openings of various shapes and sizes is presented as a plot of the Vierendeel parameter, v_i, against the critical opening length ratio, c/d_o, for perforated sections under zero global moment (**Fig. 15**).

As the ratio of the critical opening length to the web opening depth increases the Vierendeel parameter also increases (closer to unity). However, this trend does not apply to all perforated beams, especially when the diameters of the web openings, d_o, are equal to $0.5h$ and $0.65h$. **Fig. 15** shows that the Vierendeel mechanism is strongly present for perforated sections with elongated web openings. Whereas, Vierendeel action can be ignored when perforated sections with elliptical web openings are considered, i.e. $v_i < 0.2$. Perforated sections with standard typical web openings are categorized as mid-range among the FE analyses in terms of Vierendeel parameter. The logarithmic trend lines are also plotted together with their corresponding formulas, in order to be able to anticipate the importance of the Vierendeel mechanism in perforated beams with web openings of different critical opening length.

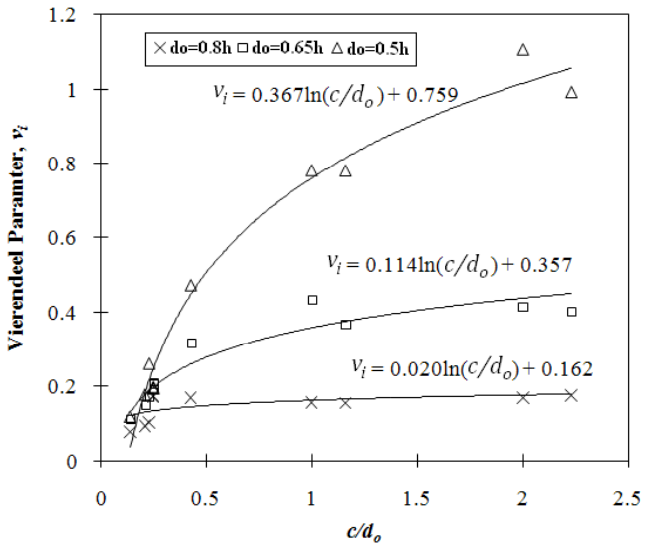

Fig. 15: Typical values for Vierendeel parameter

Generalized non-dimensional V/M interaction design curves

A generalized non-dimensional shear-moment interaction curve is presented herein. This is a non-linear interaction curve which can be used to allow for an interaction between the shear force and the moment in perforated beams as examined (i.e. with rectangular plates). Proposed design curves are drawn for each particular case.

For $\bar{v} \geq 0.72\ from\ Table\ 2 \rightarrow\ the\ design\ ratio\ is:\ \bar{\bar{v}} = \bar{v}(1 - m^z)^{\,k}$ (10)

For $\bar{v} < 0.72\ from\ Table\ 2 \rightarrow\ the\ design\ ratio\ is:\ \bar{\bar{v}} = \bar{v} - q + q(1 - m^z)^{\,k}$ (11)

The q, z and k factors, can be explicitly taken from **Table 5**. The combination of the factors is not unique, however good agreement between the design curves and the FEM curves is achieved. For convenience, the web opening types are categorized to minimize the number of factors. The 'coupled' shear capacity ratio, $\bar{v}$, should always be higher than the design 'coupled' shear ratio, $\bar{\bar{v}}$, for conservative reasons and safe design. When the 'coupled' shear capacity ratio, $\bar{v}$, has a negative value, it is considered to be zero.

Table 5: Summary of the factors for all perforated sections

A conservative design has been adopted for the non-standard elliptical web openings and particularly for the perforated sections with extreme web opening depths d_o equal to *0.8h* and *0.5h*, as current knowledge is limited. Also, conservatism is well established at the elongated web openings and particularly for the perforated sections with a web opening depth d_o equal to *0.8h*. This is because the trend of the FEM curves differs considerably for

perforated sections of the particular opening type and their large opening length makes the perforated sections vulnerable to high loads.

The following simple design steps, evaluating and assessing the Vierendeel capacity of perforated sections using any web opening shapes and sizes presented earlier, are listed below:

1. Determine the moment, $M_{o,Rd}$, (**Eqs. (4)**) and shear, $V_{o,Rd}$, (**Eqs. (3)** and **Eqs. (8)**) capacities of the perforated sections.
2. Determine the applied moment, M_{Sd}, (**Eqs. (2)**) and applied shear force, V_{Sd}, (**Eqs. (1)**) at the center-line of the web openings.
3. Find the appropriate 'coupled' shear capacity ratio, $\bar{v}$. from **Table 2**.
4. Insert $\bar{v}$ in **Eqs. (10)** or **Eqs. (11)** and by using the suitable combination of the q, z and k factors from **Table 5**, determine the design 'coupled' shear ratios,$\bar{\bar{v}}$, at any moment utilization ratio, $m=M_{Sd}/M_{o,Rd}$. In the case $\bar{\bar{v}} \leq 0$, then it is assumed that $\bar{\bar{v}} = 0$ and a lower m ratio should be examined, as the perforated section has failed by excessive applied moment.
5. Then multiply the design 'coupled' shear ratio, $\bar{\bar{v}}$, with the shear capacity of the perforated section, $V_{o,Rd}$.
6. Compare the latter result with the applied shear force, V_{Sd}, at the center-line of the web opening; the following equilibrium should be satisfied: $\bar{\bar{v}}\, V_{o,Rd} \geq V_{Sd}$). In the case that the previous equilibrium is not qualified, providing that the error is not greater than 5%, the results can be used normally. This is an outcome from the averaging of the design curve to fit the FEM results. An extended table of the q, z and k factors for all perforated sections (instead of **Table 5**) is provided by Tsavdaridis (2010), so as the design curves perfectly fit the FEM curves.

Otherwise, the 'coupled' shear ratios can be directly picked from **Fig. 8**. In this case, the 'coupled' shear capacity ratios should be multiplied by the shear capacity, $V_{o,Rd}$, and compare the result with the applied shear force, V_{Sd}.

Limitations and recommendations

This FE study is limited to typical mid-range UB perforated sections. Also, it should be clearly noted that a web opening diameter d_o equal to $0.8h$ (instead of $0.75h$) is used in this research programme aiming at lighter steel beams, or simply a more conservative design can be achieved using web openings with d_o equal to $0.75h$.

Following an overall check of all eleven web opening shapes, it can be seen that perforated sections with non-standard vertical and inclined elliptical web openings behave more effectively compared to standard circular and hexagonal web openings, mainly in terms of stress distribution. This was anticipated especially for vertical elliptical web openings as the web opening length, c, is very narrow and the web opening depth remains the

same. Also, elliptical web openings provide smooth opening edges that avert the formation of plastic hinges at a low load level. Therefore, instead of using only circular and hexagonal web openings, elliptical web openings can be also used in construction and they are especially advantageous when they are located at critical positions along the length of the beams. Moreover, more holes can be fitted along a certain length without compromising the weight of the beam (light-weight beams), whilst another comprehensive experimental and FE study (Tsavdaridis and D'Mello 2011) has shown than the new web-post between two closely spaced web openings of elliptical shapes are also stiffer and behave better under a complex failure mode.

Although the results obtained from **Fig. 8** and **Table 2** are non-dimensionalized, an overall estimation indicates that perforated sections with vertical elliptical web opening shapes (C) have a percentage improvement in terms of the 'coupled' shear capacity ratio compared to the perforated beams with standard typical circular (A) and hexagonal (B) web opening shapes. These are approximately 18.5% and 29% respectively, for the biggest web opening sizes. The above percentages are lower when inclined elliptical web opening shapes are compared to the circular and hexagonal web opening shapes as they have a wider critical opening length, c. Similarly, the above percentages are decreased when perforated beams with smaller web opening sizes are considered.

In general, the comparison could have been focused mainly amongst perforated sections with web opening shapes A to G. For instance, perforated beams with slightly different web opening areas (eg. 5.8% difference between A and G) can result different shear capacities due to the shape of the web openings (eg. **Table 2**; A and G when $d_o=0.5h$). On the other hand, at large web openings, where the critical opening length at the top and bottom tee-sections is the dominant parameter, the previous mentioned beams with similar critical opening lengths, $c=0.23d_o$ and $c=0.21d_o$ respectively, have similar 'coupled' shear capacity ratios (eg. **Table 2**; A and G when $d_o=0.8h$).

Similarly, perforated sections with D, E and F web opening shapes have different 'coupled' shear capacities (eg. $d_o=0.65h$), whilst they do have the same web opening area and critical opening length. This is happening as the rotation of the web openings differs and so the combination of forces result the deviation on their shear capacities.

The main outcome of this research programme is that the critical opening length, c, the opening depth, d_o, but also the actual web opening shape affect radically the capacities of perforated beams. This is the main reason that a wide study on web opening shapes is under serious consideration by the authors of this research paper, as opposed to the typical but currently acceptable approach, which considers only the effective web opening area in the estimation of the second moment of area and the proportionate stiffness of the reduced section along the beam. The effective web opening area of typical web opening shapes A and B is verified; however there is a

serious underestimation of the shear capacities of the perforated sections, particularly for those with thick flanges, when compared with the FE model. The effective web opening area for perforated beams with various shapes and sizes of web openings can now be estimated accurately. It is also interesting to compare FEM curves with other simple empirical interaction curves, such as the straight line and the quadratic curve, as they are widely used nowadays for the design of perforated beams. The straight line may be too conservative, whilst the quadratic curve may overestimate the results significantly.

Concluding remarks

A comprehensive FE investigation on perforated beams with circular and novel non-standard web opening shapes was carried out. The FE model was validated against experimental work found in the literature and presented herein. Analyses of perforated sections with different standard and novel non-standard web opening configurations show how the Vierendeel mechanism is affected not only by the size, but also by the shape of the web openings. More analytical the effects of the flange and web thicknesses, the critical web opening length and depth as well as the web opening shape are presented through a parametric FE investigation. The investigation on novel elliptical web openings presents some positive results and others that update current knowledge. Based on the FE model, improvements to the assessment of load carrying capacities of steel beams with large web openings are obtained by careful observation of plastic hinge formation at both the LMS and the HMS of the perforated sections, followed by load redistribution across the web opening at large deformation. The method of using the shear-moment interaction curves was widely used in the past, but the methodology is now enhanced by a comprehensive FE study. The proposed method is shown to be conservative and efficient in terms of structural adequacy and calculation effort when compared with the use of FE modeling. As a result, simple design rules were developed for engineers in their general practice. Further, the outcome of this research can be effectively applied in various engineering fields, enhancing the structural behavior of perforated structural forms, without adding stiffeners or taking other strengthening precautions, and prevent local instability due to high stress concentration at specific locations in the vicinity of the web openings, by better understanding of the failure mechanisms. The FEA provides a good tool for the prediction of the Vierendeel loads and the results can be very applicable.

References

Altifillisch M.D., Cooke B.R. and Toprac A.A. (1957) “An investigation of open web expanded beams.” *Welding Research Council Bulletin*, New York, Series No.47, pp. 307-320

Bower J.E. (1968) “Design of beams with web openings.” *Journal of the Structural Division*, Proceedings of the American Society of Civil Engineers

BS5950 Part 1:2000 (2000) “Structural Use of Steelworks in Building. Code of practice for design, Rolled and welded sections.” *BSI*

Chung K.F., Liu T.C.H. and Ko A.C.H. (2000) “Investigation on Vierendeel mechanism in steel beams with circular web openings.” *Journal of Constructional Steel Research*, 57, pp. 467-490

Chung K.F., Liu T.C.H. and Ko A.C.H. (2003) “Steel beams with large web openings of various shapes and sizes: an empirical design method using a generalized moment-shear interaction.” *Journal of Constructional Steel Research*, 59, pp. 1177-1200

Darwin D. (1990) “Steel and composite beams with web openings.” *In: Steel Design Guide Series No.2*, Chicago, IL, USA: American Institute of Steel Construction

ENV 1993-1-3 (1998) “EC3: Design of steel structures: Part1.1. General rules and rules for buildings 1992, and Amendment A2 of Eurocode 3: Annex N Openings in webs.” BSI

Lawson R.M. (1987) “Design for openings in the webs of composite beams.” *CIRIA/Steel Construction Institute*, CIRIA Special Publication and SCI Publication 068

Oehlers D.J. and Bradford M.A. (1995) “Composite steel and concrete structural members: Fundamental behaviour.” Pergamon

Redwood R.G. (1969) “The strength of steel beams with unreinforced web holes.” *Civil Engineering and Public Works Review*

Redwood R.G. (1973) “Design of beams with web holes.” *Canadian Steel Industry Construction Council*, Willow dale, Ontario, Canada

Redwood R.G. and McCutcheon J.O. (1968) “Investigation on Vierendeel mechanism in steel beams with circular web openings.” *Journal of Structural Division*, Proc ASCE, 94(ST1):1-17

Redwood R.G. and Cho S.H. (1993) “Steel and composite beams with web openings.” *In: Steel Design Guide Series No.2*, Chicago, IL, USA: American Institute of Steel Construction

Toprac A.A. and Cooke B.R. (1959) "The plastic behavior of castellated beams." *Welding Research Council Bulletin*, New York, Series No.47, pp. 1-10

Tsavdaridis, K.D. and D'Mello, C. (2009) "Finite element investigation of perforated steel beams with different web opening configurations." *6th International Conference on Advances in Steel Structures* (Hong Kong China December 16-18, 2009) ICASS'09/IJSSD/IStructE Asia-Pacific Forum, Hong Kong, China, pp. 213-220

Tsavdaridis, K.D. (2010) "Structural performance of perforated steel beams with novel web openings and with partial concrete encasement." PhD Thesis (supervised by Dr. C. D'Mello), School of Engineering and Mathematical Sciences, City University, London

Tsavdaridis, K.D. and D'Mello, C. (2011) "Behavior and Strength of Perforated Steel Beams with Novel Web Opening Shapes." *The Journal of Constructional Steel Research*, 67, pp. 1605-1620

Notation

A_v or A_{VZ}	Shear area of the un-perforated section
A_{vo}	Reduced shear area of perforated section
c	Critical opening length
d_o	Diameter of the web opening
h	Overall depth of the steel beam
L	Span of the specimen
m	Moment utilization ratio
$\overline{m}$	'Coupled' moment capacity ratio
$M_{o,Rd}$	Moment capacity of the perforated section
$M_{o,Sd(FEA)}$	Global 'coupled' moment capacity of perforated sections as obtained from FEA
M_{Sd}	Global bending moment at center-line of the web opening
$M_{T,Rd}$	Basic shear capacity of the tee-sections under zero axial and shear forces
M_{φ}	Local bending moment at the angle, φ, of the first plastic hinge at the top tee-section and LMS
$P_{cr.}$	Critical load
$P_{ult.}$	Ultimate load
P_v	Shear capacity of steel un-perforated sections
r	Root radius of steel UB section
v	Shear utilization ratio
$\bar{v}$	'Coupled' shear capacity ratio
$\bar{\bar{v}}$	Design 'coupled' shear ratio

v_i	Vierendeel parameter
$V_{o,Rd}$	Shear capacity of the perforated section
$V_{o,Sd(FEA)}$	Global 'coupled' shear capacity of perforated sections as obtained from FEA
V_{Sd}	Global shear force at center-line of web opening
w	Failure load from the FE model (N/mm)
W_{pl}	Plastic modulus of the overall section
x	Web opening positions along the beam
γ_{Mo}	Partial safety factor taken as 1.0 for conservative design purposes
φ_p	Formation of a plastic hinge at a cross-section announces that the actions on the section are large whilst the capacities are not

Tables

Measured Material Strengths		Beam 2A	Beam 3A
Flanges	Yield Strength, f_y (MPa)	352	311
	Tensile Strength, $f_{ult.}$ (MPa)	503	576
Web	Yield Strength, f_y (MPa)	376	361
	Tensile Strength, $f_{ult.}$ (MPa)	512	492

Table 1: Material properties of the steel beams taken from coupon tests

Opening Types	Opening Shapes	Opening Length, *c*	Max. 'Coupled' Shear Capacity Ratios, $\bar{v}$ ($M_{Sd}/M_{o,Rd}=0$)					
			0.44h*	***0.5h***	***0.57h****	***0.65h***	***0.7h****	***0.8h***
Standard Typical	**A**	$0.23d_o$	-----	0.95	-----	0.86	-----	0.75
	B	$0.423d_o$	-----	0.92	-----	0.82	-----	0.65
Non-Standard Elliptical	**C**	$0.14d_o$	-----	0.71	-----	0.88	-----	0.92
	D	$0.25d_o^*$	0.60	-----	0.79	-----	0.88	-----
	E	$0.25d_o^*$	0.59	-----	0.78	-----	0.87	-----
	F	$0.25d_o^*$	0.59	-----	0.72	-----	0.87	-----
	G	$0.21d_o$	-----	0.71	-----	0.79	-----	0.74
Standard Elongated	**H**	$1.0d_o$	-----	0.65	-----	0.48	-----	0.26
	I	$1.16d_o$	-----	0.56	-----	0.35	-----	0.22
	J	$2.0d_o$	-----	0.46	-----	0.23	-----	0.14
	K	$2.23d_o$	-----	0.37	-----	0.20	-----	0.13

**New web opening depth for rotated inclined elliptical web opening*

Table 2: Summary of maximum 'coupled' shear capacity ratios, $\bar{v}$

Section Sizes	Opening Shapes	Opening Size d_o/h	t_f/t_w	t_w/h	**BS** $\bar{v}$ ratio	**EC3** $\bar{v}$ ratio	**Eqs. (8)** $\bar{v}$ ratio	**BS** vs. **EC3** (%)	**BS** vs. **Eqs. (8)** (%)	**EC3** vs. **Eqs. (8)** (%)
UB 610x229x140	A	0.8	1.69	0.021	1.11	0.90	0.77	18.9	30.6	14.4
	C				1.47	1.17	1.02	20.4	30.6	12.8
	I				0.76	0.62	0.53	18.4	30.3	14.5
UB 610x229x101	A	0.8	1.41	0.017	0.96	0.76	0.78	20.8	18.8	2.56
	C				1.27	0.98	1.01	22.8	20.5	2.97
	I				0.47	0.39	0.39	17.0	17.0	0.00
UB 457x152x82	A	0.8	1.80	0.022	1.17	0.93	0.77	20.5	34.2	17.2
	C				1.42	1.12	0.93	21.1	34.5	16.9
	I				0.77	0.60	0.44	22.1	42.8	26.6
UB 457x152x52	A	0.8	1.43	0.016	0.95	0.72	0.75	24.2	21.0	4.00
	C				1.16	0.87	0.92	25.0	20.7	5.43
	I				0.27	0.20	0.22	25.9	18.5	9.09

Table 3: Comparison of the 'coupled' shear capacity ratios, $\bar{v}$

Opening Shapes	Under high shear (pos. x=2)	Under high shear and moment (pos. x=4)
	φ_p (degrees)	φ_p (degrees)
A	23 / both open.	19 / both open.
B	22 / both open.	22 / both open.
C	17 / both open.	14 / both open.
D	16 / both open.	8 / both open.
E	33 / both open.	31 / both open.
F	34 / left open. 14 / right open.	32 / left open. 9 / right open.
G	32 / left open. 11 / right open.	29 / left open. 7 / right open.
H	41 / both open.	41 / both open.
I	49 / both open.	49 / both open.
J	60 / both open.	59 / both open.
K	64 / both open.	64 / both open.

Table 4: Angle, φ_p, of the first plastic hinge at top tee-section and LMS following load redistribution

Initial Web Opening Depth, d_o		*0.5h*			*0.65h*			*0.8h*		
Factors		*q*	*z*	*k*	*q*	*z*	*k*	*q*	*z*	*k*
Web Opening Shapes	**A**	-----	2.50	0.30	-----	1.30	0.30	-----	1.80	0.30
	B	-----	2.00	0.30	-----	1.00	0.30	0.70	1.50	0.40
	C	1.40	2.00	0.50	-----	2.00	0.70	-----	1.20	0.20
	D	1.40	2.00	0.45	-----	1.70	0.80	-----	1.00	0.20
	E	1.40	2.00	0.45	-----	1.60	0.60	-----	0.80	0.20
	F	1.40	2.00	0.45	-----	1.00	0.20	-----	1.10	0.20
	G	1.20	2.00	0.40	-----	1.60	0.30	-----	1.70	0.20
	H	0.70	1.50	0.60	0.50	3.50	0.40	0.50	1.60	0.40
	I	0.70	1.50	0.60	0.40	2.00	0.30	0.50	1.60	0.35
	J	0.50	2.50	0.70	0.50	2.00	0.30	0.80	3.00	1.10
	K	0.50	2.00	0.20	0.50	3.50	0.55	0.80	3.00	1.50

Table 5: Summary of the factors for all perforated sections